DOI 10.1007/s10812-022-01343-3
Journal of Applied Spectroscopy, Vol. 89, No. 1, March, 2022 (Russian Original Vol. 89, No. 1, January–February, 2022)

A NOVEL TURN-ON THE FLUORESCENCE SENSOR FOR H_2S AND ITS APPLICATIONS IN BIOIMAGING

Y. Yan, Sh. Zhu, Zh. Chen, and Y. Ji* UDC 535.372

A fluorescent probe II, 6-azido-2-(2-hydroxyethyl)-1H-benzo[de]isoquinoline-1,3(2H)-dione with specific identification environment H_2S, was designed and synthesized based on 4-bromine-1,8-naphthalimide and ethanamine. We used 4-bromine-1,8-naphthimide as raw materials to synthesize a new type of reactive fluorescent probe based on the mechanism of intramolecular charge transfer. These two materials are easily obtainable, low in cost, and can be synthesized through a simple two-step reaction. 1,8-Naphthalene anhydride has a moderate fluorescent ability as it introduces an electron-donating group at position 4. A change to its conjugate system can cause a push-pull electronic effect in the molecule and result in a very strong luminous effect. The structure of probe II was characterized by IR, ESI, and NMR. The preliminary screening was under the UV lamp. We found that probe II had a certain specific recognition effect on H_2S in the DMSO solvent. After the solvent screening, DMSO was selected as a solvent to identify H_2S specifically for the probe. The fluorescence spectroscopy illustrated that probe II showed green fluorescence in the DMSO solution. With the continuous addition of H_2S, probe II showed red fluorescence at 510 nm, which produced a strong fluorescence emission peak that stood out from the rest of the spectrum. The experimental results showed that the probe had a very good sensitivity at detecting H_2S (with a minimum concentration of 1×10^{-7} mol/L). Meanwhile, dozens of cations and anions do not interfere with the recognition of H_2S by the probe molecule in the DMSO system. At the same time, we found that probe II could also recognize H_2S by cell imaging technology.

Keywords: *fluorescence probe, hydrogen sulfide, intramolecular charge transfer.*

Introduction. Hydrogen sulfide is an important endogenous gaseous compound that plays an important role in cells. In addition to nitric oxide and carbon monoxide, it is considered to be the third most important gas that regulates the cardiovascular, neuronal, immune, endocrine, and gastrointestinal systems [1, 2]. Hydrogen sulfide possesses different characteristics and plays different physiological roles such as mediation of neurotransmission [3], cardioprotection [4], modulation of blood pressure [5], and exertion of anti-inflammatory effects. Endogenous H_2S was mostly biosynthesized from cysteine or cysteine derivatives by three distinctive enzymes, including cystathionine-β-synthase (CBS), cystathionine-γ-lyase (CSE), and 3-mercaptopyruvate sulfurtransferase (3-MST) in mitochondria or cytosol [6, 7]. These enzymes are found in a variety of biological cells and tissues, and their expression can be induced by a variety of diseases [8, 9]. Endogenous H_2S can also be produced by nonenzymatic methods, such as a spontaneous reaction of reduced glutathione (GSH) with sulfur to produce H_2S. Meanwhile, the iron-sulfur cluster contains another nonenzymatic protein carrying Fe_2S_2, Fe_3S_4, or a Fe_4S_4 cluster protein promoting H_2S source [10, 11]. To understand the roles of H_2S in a biological system, the development of new convenient and efficient detection methods for detecting H_2S is required. Typical instrumental techniques, including spectrophotometric [12] and electrochemical assays [13], gas chromatography analysis [14], and sulfur chemiluminescence detection [15], have been used to monitor H_2S. However, these methods are limited in accuracy. So, a variety of novel detection methods have been developed [16–25]. Among them, the most promising is based on using fluorescent probes. Recently, several fluorescent probes have been reported to detect H_2S in living systems [26–29]. Common strategies include the H_2S mediated reduction of azide to amine [30, 31]. H_2S is trapped by nucleophilic addition [32, 33], copper sulfide precipitation [34, 35], and thiolysis of dinitrophenyl ether [36, 37]. Fluorescent probes based on these strategies usually utilize the dual nucleophilicity of H_2S.

*To whom correspondence should be addressed.

Guangdong Provincial Key Laboratory of Quantum Engineering and Quantum Materials School of Physics and Telecommunication Engineering at South China Normal University, Guangzhou, China; email: jiyh@scnu.edu.cn. Abstract of article is published in Zhurnal Prikladnoi Spektroskopii, Vol. 89, No. 1, p. 139, January–February, 2022.

In recent years, the design of fluorescent probes for hydrogen sulfide has mainly used the unique chemical properties of hydrogen sulfide, such as dual nucleophilicity, reducibility, and complexation with copper ions. The dual nucleophilicity of hydrogen sulfide has good prospects in the design of hydrogen sulfide molecular probes, but there is an unavoidable problem in the hydrogen sulfide probe molecules designed using dual nucleophilicity, namely, although the probe molecules are not affected by cysteine biological thiols such as acid and glutathione interfere, they are easily consumed by biological thiols. As a result, they cannot be used in vivo. In addition, the detection limit of most probes is 10^{-4} mol/L. The dual nucleophilicity, as the name suggests, means that hydrogen sulfide can nucleophilically attack the probe molecule twice. Although cysteine and glutathione can react with the probe molecule, they cannot perform a second nucleophilic attack. The probe we designed cannot be interfered by other biological thiols, anions, and cations, and has an obvious color reaction under visible light.

On the basis of previous technologies, a new probe was designed and synthesized. The probe, which can detect H_2S, was based on 4-bromine-1,8-naphthalimide and ethanamine. This probe has better water solubility, simple synthesis steps, and small interference between anions and cations. After a series of tests, we have obtained a probe that emits yellow fluorescence under the excitation of a UV lamp. Through further research, we found that this probe can be used for the selective and sensitive detection of H_2S. All the results were fully tested by IR, ESI, and NMR.

Experimental. 4-Bromine-1,8-naphththalimide and ethanamine and sodium azide were purchased from Shanghai. The salts solutions of metal ions, such as NaCl, KCl, $MgCl_2{\cdot}6H_2O$, $CaCl_2$, Na_3PO_4, NaH_2PO_4, $NaHCO_3$, $NaNO_3$, $Na_2C_2O_4{\cdot}H_2O$, Na_2HPO_4, $NaNO_2$, $NaAC{\cdot}H_2O$, NaBr, $NaCO_3$, $NaSO_4$, and NaI, and GSH and Gly were purchased from Shanghai Experiment Reagent Co, Ltd (Shanghai, China). All the other chemicals used were of analytical grade. Deionized water was used to prepare all aqueous solutions.

Scanning in the range of 4000–400 cm^{-1} was performed on a Shimadiu-FTIR-8300 Fourier transformation infrared spectrometer (KBr tablet) to measure the infrared spectrum. The hydrogen nuclear magnetic resonance spectrum and the carbon nuclear magnetic resonance spectrum were measured on an AVANCE III HD nuclear magnetic resonance spectrometer produced by Bruker in Switzerland. Mass spectrometry was performed on an AB 5600 MALDI-TOF ultra-high resolution time-of-flight mass spectrometer produced by AB SCIEX, The proton nuclear magnetic resonance spectrum and the carbon nuclear magnetic resonance spectrum supplemented by infrared spectroscopy and mass spectrometry were used to verify the consistency of the probe with the expected design structure, and mass spectrometry analysis was used to verify the postulated recognition mechanism. Using Gaussian16 (DFT-B3LYP-6-31G*), we calculated the HOMO–LUMO Gap of original state II and reduced state III.

The synthesis of II is summarized in Scheme 1. To a 100-mL flask we added 2 g (7 mmol) of 4-bromine-1,8-naphthalimide into 65 mL of DMF until they completely dissolved. Sodium azide (1.85 g, 28 mmol) dissolved in 3 mL of pure water was slowly dripped into the flask. The color of the solution changed to a dark brown. The reaction proceeded for 6 h at 50°C. After that we put the reaction mixture into an ice–water mixture until mass precipitation appeared. We filtered and dried them in the air. A total of 1.8 g of yellow–green powder was obtained. The above-mentioned compounds were dissolved in 65 mL of ethyl alcohol. We added 0.0.625 g (10 mmol) of ethanolamine into the solution and heated it up to reflux. The final product was obtained. The dark yellow crystal was recrystallized from the ethyl alcohol at room temperature.

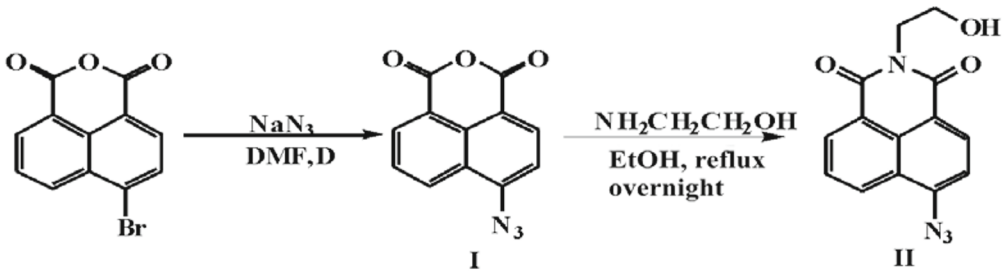

Scheme 1. Synthesis of probe II.

IR (cm^{-1}, s strong, m medium, w weak): 1697.21s, ν(C=O), 2132.95s, ν(N≡N). ^{1}H-NMR(400MHz, DMSO) δ 7.89–7.85 (m, 2H), 7.81 (d, *J* = 4.4 Hz, 1H), 7.69 (d, *J* = 8.5 Hz, 1H), 7.44 (t, *J* = 7.4 Hz, 2H), 7.39 (t, *J* = 7.2 Hz, 1H), 6.83–6.79 (m, 2H), 6.77 (ddd, *J* = 8.1, 6.0, 1.8 Hz, 1H), 4.49–4.43 (m, 1H), 4.26–4.17 (m, 2H), 4.14–4.08 (m, 2H), 2.45 (s, 3H). ^{13}C-NMR (101MHz, DMSO) δ 163.73 (s), 163.20 (s), 143.09 (s), 131.80 (d, *J* = 11.8 Hz), 128.57 (s), 127.59 (s), 123.69 (s), 122.52 (s), 118.54 (s), 116.29 (s).

The fluorescence spectrum and UV-Vis procedures were performed in a quartz optical cell of 1.0 cm optical path length at room temperature. All fluorescence measurements were performed under 420 nm excitation; the slit width was 3 nm/3nm. The fluorescence procedures were as follows: Ions were slowly added into DMSO containing 1.0 μM of the probe; then the titration experiment and the interference experiment were carried out. In the experiment on the UV-vis spectra, a 20 μM probe was prepared in a quartz cell containing DMSO, and 1×10^{-2} mol/L H_2S was gradually added. After adding the ions, we recorded all the fluorescence spectra and the UV-vis data.

In a humid environment containing 5% CO_2, we cultivated SiHa in DMEM with 10% fetal bovine serum, and then a subculture with 0.05% trypsin at 37°C in a 35 × 35 mm glass Petri dish. After waiting for 24 h, the probe solution was aspirated, the cells were washed three times with PBS, mounted with 50% glycerol, and then observed with a laser confocal fluorescence microscope.

Firstly, we cultured SiHa cells with probe II (10 μM) for 30 min. Secondly, the SiHa cells were cultured with probe II (10 μM) for 30 min, and then H2S (40 μM) was added and the whole cultured for 30 min. Lastly, we also cultured SiHa cells for 30 min, then put H_2S (40 μM) and cultured it for 30 min.

The cytotoxicity of probe II was assessed in SiHa cells with a CCK-8 kit (Dojindo). In brief, the cell density was 10000/well, cultured for 24 h, and then checked. Then probe II was added to it. The medium was removed after 24 h, 10 μL of the CCK-8 reagent was added to each, and a temperature of 37°C was set for 1 h. Absorbance values were measured at 450 nm using a SpectraMax® M5 microplate reader (Molecular Devices, WI, USA). The experiment was repeated five times for each sample.

We calculated the probe and the state when the probe was combined with hydrogen sulfide on Gaussian16. Moreover, we calculated the HOMO–LUMO gap of the original state and the reduced state.

Results and Discussion. As shown in Scheme 1, the probe was designed and synthesized. Its chemical structure was proved by ^{1}H NMR, ^{13}C NMR, infrared spectroscopy (IR), and electrospray ionization mass spectra (ESI–MS) (Figs. S1–S4).

In order to verify the probe's ability to detect H_2S at room temperature, we put 0.8 μL of the probe solution with 1.0×10^{-2} mol/L concentration into a cuvette containing 2 mL of DMSO and then gradually added dropwise the sodium sulfide solution (concentration 2×10^{-4} mol/L, 0.5 μL added each time). As shown in Fig. 1, as the amount of Na_2S continues to increase, the fluorescence intensity at 530 nm gradually increases, and the color of the fluorescence gradually changes from bright yellow to purple. It can be seen that in the DMSO system the probe can specifically recognize hydrogen sulfide.

We added 20 μL of the DMSO solution with concentration 1.0×10^{-2} mol/L of probe molecules to a quartz cuvette containing 2 mL of analytically pure ethanol, and then gradually added the 2.0×10^{-4} mol/L Na_2S solution. As shown in Fig. 2, as the concentration of the Na_2S solution gradually increases, the broad absorption peak at 330–390 nm gradually weakens, and the broad absorption peak at 410–500 nm gradually increases. When the concentration of Na_2S in the system reaches 3.2×10^{-6} mol/L, the intensity of the absorption peaks no longer changes. With increase in the Na_2S concentration, the color of the system changes from golden yellow to purple.

We also explored whether the probe's recognition of hydrogen sulfide in the DMSO system is interfered by the presence of anions and cations in the living system. We screened 18 anions and cations. We added 2 mL of analytically pure DMSO to the quartz cuvette, then used a pipette to add 0.8 μL of the probe with a concentration of 1.0×10^{-2} mol/L. The fixed excitation wavelength was 420 nm, and the slit width 3 nm/3 nm. We got the maximum emission wavelength and added 0.5 μL of 1.0×10^{-4} mol/L of ions into the system to obtain the change value of the maximum emission wavelength. The results of the experiment are shown in Figs. 3 and 4. The probe molecule is for the detected anions and cations such as Br^-, Cl^-, CO_3^-, Ca^{2+}, Mg^{2+}, K^+, NO_3^-, HCO_3^-, $H_2PO_4^-$, PO_4^{3-}, SO_4^{2-}, I^-, GSH, Gly, AC^-, HPO_4^{2-}, $C_2O_4^{2-}$, and NO_2^-. The probe has no obvious response signal to the above-mentioned ions. At the same time, we also explored whether the above interfering ions interfere with the visual recognition of hydrogen sulfide in the probe. We added about 1.5 mL of DMSO and 1.0×10^{-2} mol/L of the probe to each small sample bottle. The probe molecule is 1.0 μL, and the above-mentioned ions to be screened are added to each sample bottle. After shaking evenly, we placed them under visible light and ultraviolet light for observation. We found that under visible light and ultraviolet light, anions, cations, and biothiols (cys) show significant interference to the probe molecule, and under visible light, a small amount of hydrogen sulfide can cause a strong color change in the DMSO solution of the probe molecule, which shows that probe II is good at visual recognition of hydrogen sulfide with great application prospects.

Cellular imaging. The ultimate goal of the synthetic fluorescent probe is its application in biological systems. In order to measure the probe's ability to detect H_2S in living cells at 37°C, we used a LeicaTCS, SP5 laser scanning

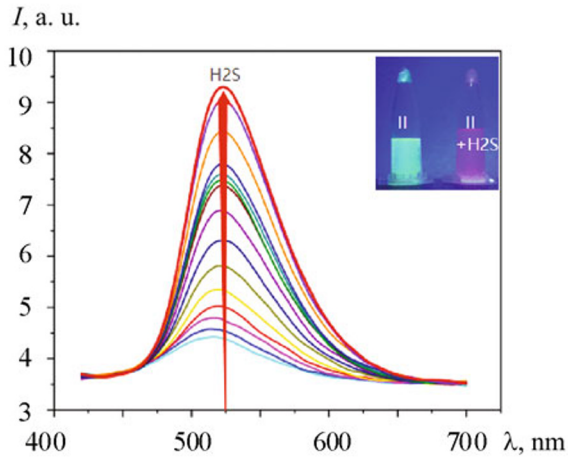

Fig. 1. Fluorescent spectral changes of probe II (4 μM) upon addition of Na_2S (0, 0.05, 0.10, 0.15, 0.20, 0.25, 0.30, 0.35, 0.40, 0.45, 0.50, 0.55, 0.60, 0.65, and 0.70 μM) in DMSO at room temperature. Inset: the visible fluorescence changes upon UV irradiation.

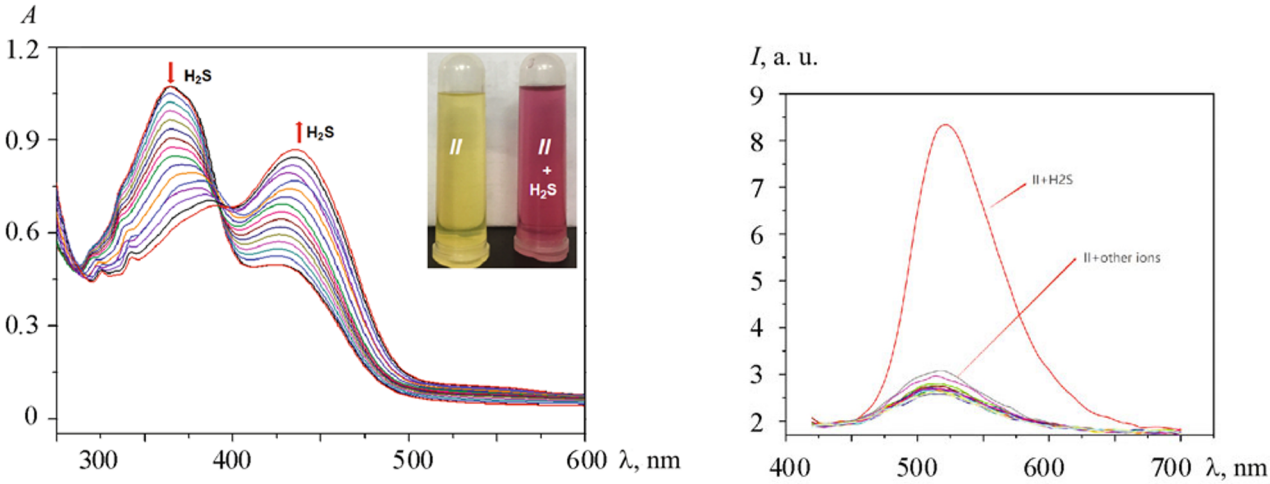

Fig. 2. UV-Vis spectra of probe II upon addition of Na_2S in DMSO at room temperature. Inset: The visible fluorescence changes upon UV irradiation.

Fig. 3. Fluorescence response of probe II upon the addition of several ions in DMSO.

microscope to obtain laser confocal fluorescence imaging. Then we put SiHa cells in the probe and incubated it for 30 min, and then added H_2S to the system and continued to incubate it for 30 min. As shown in Fig. 5, the probe of the cell system shows green fluorescence under the induction of laser copolymerization when there is no H_2S. The cells show obvious red fluorescence, the cell penetration of the probe, and the fluorescence ability in the cell when H_2S is added to the cell system for culture. This result shows the prospect of the probe's bio-utilization.

In order to further prove the potential application of probe II in living cells, we applied it to SiHa cells for fluorescence imaging. Since the cytotoxicity of probe II is the main consideration for its biological application, the cytotoxicity study of probe II was carried out on SiHa cells by the CCK-8 kit. As shown in Fig. 6, the cell viability decreases slightly while the concentration of probe II increases (0, 4, 8, 16, 32, and 60 μM). When the concentration of probe II is 60 μM, the viability of the cells is about 80% of its initial value, indicating that the cytotoxicity of probe II is relatively low, thus beneficial for the biological imaging subject.

Computational simulation. As shown in Fig. 7, we used Gaussian16 (DFT-B3LYP-6-31G*) to calculate the HOMO–LUMO gap of original state II and reduced state III. It can be seen that the HOMO–LUMO gap (9.3559 eV) of the original

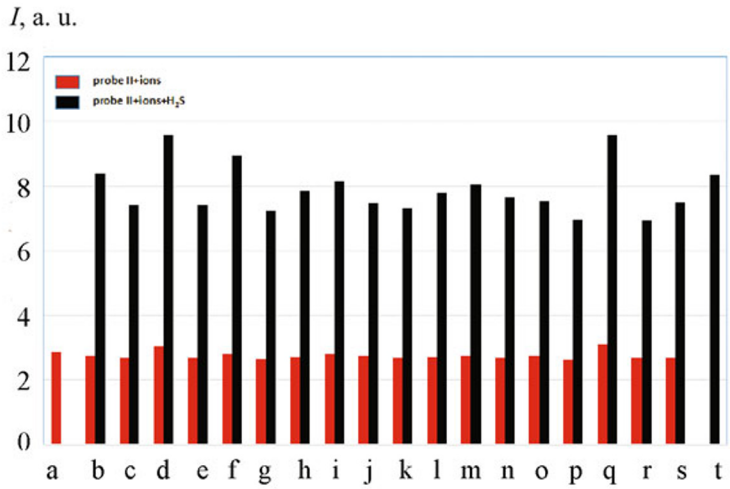

Fig. 4. Fluorescence intensity of probe II (a) and its reaction with H_2S in the presence of various ions in DMSO. λ_{ex} = 420 nm, slit: 3 nm/3 nm. b) Br^-; c) Cl^-; d) CO_3^-; e) Ca^{2+}; f) Mg^{2+}; g) K^+; h) NO_3^-; i) HCO_3^-; j) $H_2PO_4^-$; k) PO_4^{3-}; l) SO_4^{2-} ; m) I^-; n) GSH; o) Gly; p) AC^-; q) HPO_4^{2-}; r) $C_2O_4^{2-}$; s) NO_2^-; t) probe + H_2S.

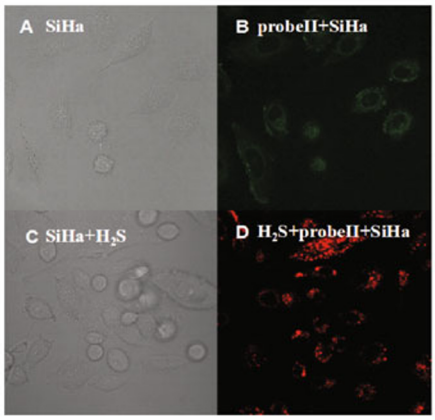

Fig. 5. Probe cells are shown as experimental results.

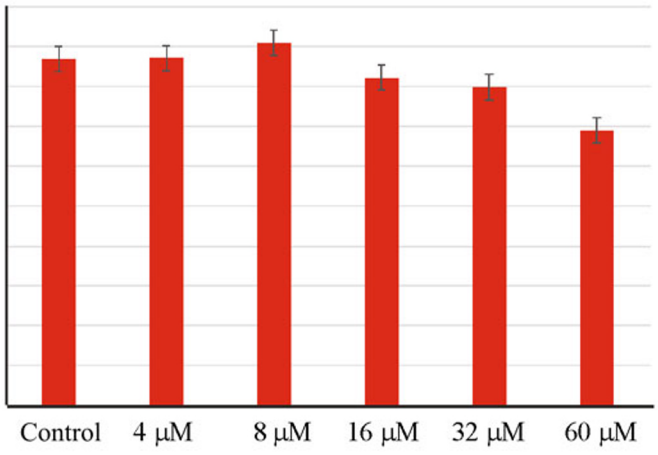

Fig. 6. Cell viability incubated with probe II at various concentrations. The experiments were repeated five times.

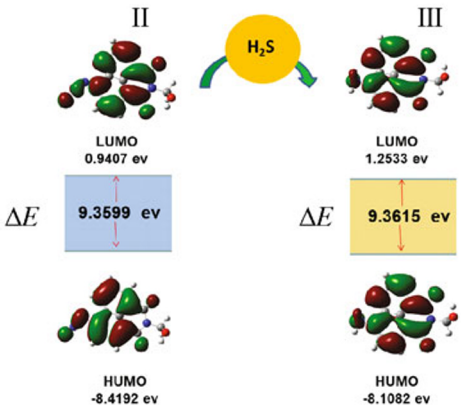

Fig. 7. HOMO–LUMO gap in original state II and reduced state III.

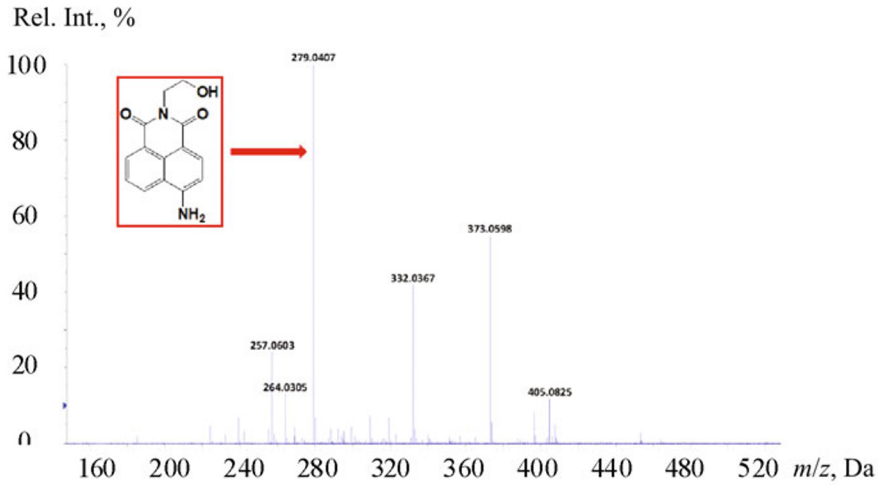

Fig. 8. Electrospray ionization mass spectrometry of the compound probe + hydrogen sulfide.

state II is smaller than the HOMO–LUMO gap (9.3615 eV) of the reduced state III. Therefore, state III is more stable than state II.

For the mechanism of the probe in recognizing hydrogen sulfide, we have made the following speculation. HS^- reduces the azide group to an amino group and is oxidized to elemental sulfur:

At the same time, this hypothesis was verified by the method of electrospray mass spectrometry. It can be seen from Fig. 8 that the molecular ion peak of the reaction product of the probe molecule and H_2S is m/z = 257.0603. This can be attributed to $[\text{compound} + H]^+$ (theoretical value 257.0926). The molecular ion peak m/z = 279.0407 can be assigned as $[\text{compound} + Na]^+$ (theoretical value 279.0746).

Conclusions. We have successfully synthesized a turn-on fluorescent probe for highly sensitive detection of H_2S with fast response time. This probe shows high selectivity for H_2S compared to other ions and has a very fast discoloration reaction. Furthermore, fluorescence imaging indicates that probe II has great potential in biological imaging. It remains stable in cells when combined with hydrogen sulfide. More importantly, the probe shows low cytotoxicity and good cell membrane permeability in the above experiments and can be used for in vivo imaging of H_2S.

Acknowledgments. This research was funded by NSFC China (Grant No. 81871395, 81571837). This work was also financially supported by the Science and Technology Program of Guangzhou (No. 201950001).

REFERENCES

1. Q. Zhao, J. Kang, Y. Wen, F. Huo, Y. Zhang, and C. Yin, *Spectrochim. Acta A*, **189**, 8–12 (2018).
2. Y. Chen, W. Yao, Y. Ding, B. Geng, M. Lu, and C. Tang, *Pulmonart. Pharmacol. Ther.*, **21**, 40–46 (2008).
3. V. S. Fernandes, A. S. Ribeiro, M. P. Martinez, L. M. Orensanz, M. V. Barahona, A. Martinezsaenz, P. Recio S. Benedito, S. Bustamante, and J. Carballido, *J. Urol.*, **189**, No. 4, 1567–1573 (2013).
4. J. W. Calvert, S. Jha, S. Gundewar, J. W. Elrod, A. Ramachandran, C. B. Pattillo, C. G. Kevil, and D. J. Efer, *Circ. Res*., **105**, No. 4, 365 (2009).
5. S. Sowmya, Y. Swathi, L. Y. Ai, L. S. Mei, P. K. Moore, and M. Bhatia, *Vasc. Pharmacol.*, **53**, No. 4, 138–143 (2010).
6. B. Renga, *Allergy Drug Targets*, **10**, No. 2, 85–91 (2011).
7. N. Shibuya, M. Tanaka, M. Yoshida, Y. Ogasawara, T. Togawa, K. Ishii, and H. Kimura, *Antioxid. Redox Signal.*, **65**, No. 4, 703–714 (2009).
8. T. S. Bailey and M. D. Pluth, *J. Am. Chem. Soc.*, **135**, 16697–16704 (2013).
9. Y. Zhao, H. Wang, and M. Xian, *J. Am. Chem. Soc.*, **133**, 15–17 (2011).
10. D. G. Searcy and S. H. Lee, *J. Exp. Zool.*, **282**, 310–322 (1998).
11. H. Beinert, R. H. Holm, and E. Munck, *Science*, **277**, 653–659 (1997).
12. M. Shariati-Rad, M. Irandoust, and F. Jalilvand, *Int. J. Environ*. *Sci. Technol.*, **13**, 1347–1356 (2016).
13. B. Li, L. Li, K. Wang, C. Wang, L. Zhang, K. Liu, et al., *Anal. Bioanal. Chem*., 1–7 (2016)
14. C. D. Pearson and W. J. Hines, *Anal*. *Chem*., **49**, 123–126 (1977).
15. M. A. H. Khan, M. E. Whelan, and R. C. Rhew, *Talanta*, **88**, 581–586 (2012).
16. A. R. Lippert, E. J. New, and C. J. Chang, *J. Am. Chem. Soc.*, **133**, 10078–10080 (2011).
17. H. Peng, Y. Cheng, C. Dai, A. L. King, B. L. Predmore, D. J. Lefer, and B. Wang, *Angew. Chem. Int*., *Ed*., **50**, 9672–9675 (2011).
18. X. Zhou, S. Lee, and Z. Xu. J. Yoon, *Chem. Rev*., **115**, 7944–8000 (2015).
19. L. Chen, D. Wu, C. S. Lim, D. Kim, S. J. Nam, W. Lee, G. Kim, H. M. Kim, and J. Yoon, *Chem. Commun.*, **53**, 4791–4794 (2017).
20. Y. L. Pak, J. Li, K. C. Ko, G. Kim, J. Y. Lee, and J. Yoon, *Anal. Chem*., **88**, 5476–5481 (2016).
21. M. D. Hartle and M. D. Pluth, *Chem. Soc. Rev*., **45**, 6107–6117 (2016).
22. Z. Yuan, F. Lu, M. Peng, C. W. Wang, Y. T. Tseng, Y. Du, N. Cai, C. W. Lien, H. T. Chang, Y. He, and E. S. Yeung, *Anal. Chem*., **87**, 7267–7273 (2015).
23. A. R. Lippert, *J. Inorg*. *Biochem.*, **133**, 136–142 (2014).
24. L. A. Montoya, T. F. Pearce, R. J. Hansen, L. N. Zakharov, and M. D. Pluth, *J. Org. Chem.,* **78**, 6550–6557 (2013).
25. L. Yi and Z. Xi, *Org. Biomaol*. *Chem.*, **15**, 3828–3839 (2017).
26. V. S. Lin and C. J. Chang, *Curr. Opin*. *Chem. Biol*., **16**, 595–601 (2012).
27. C. C. Zhao, X. L. Zhang, K. B. Li, et al., *J. Am*. *Chem. Soc*., **137**, 8490–8498 (2015).
28. X. Wang, J. Sun, W. H. Zhang, et al., *Chem. Sci*., **4**, 2551–2556 (2013).
29. Z. S. Wu, Y. L. Feng, B. Geng, J. Y. Liu, and X. J. Tang, *RSC Adv*., **4**, 30398–30401 (2014).
30. H. J. Peng, Y. F. Cheng, C. F. Dai, et al., *Angew. Chem*. *Int. Ed*., **50**, 9672–9675 (2011).
31. S. Chen, Z. J. Chen, W. Ren, and H. W. Ai, *J. Am*. *Chem. Soc*., **134**, 9589–9592 (2012).
32. K. J. Wu, G. Q. Li, Y. Li, L. X. Dai, and S. L. You, *Chem. Commun*., **47**, 493–495 (2011).
33. C. R. Liu, J. Pan, S. Li, et al., *Angew. Chem. Int. Ed*., **50**, 10327–10329 (2011).
34. C. R. Liu, B. Peng, S. Li, et al., *Org. Lett*., **14**, 2184–2187 (2012).
35. K. Sasakura, K. Hanaoka, N. Shibuya, et al., *J. Am*. *Chem. Soc*., **133**, 18003–18005 (2011).
36. F. P. Hou, L. Huang, P. X. Xi, et al., *Inorg*. *Chem*., **51**, 2454–2460 (2012).
37. X. W. Cao, W. Y. Lin, K. B. Zheng, and L. W. He, *Chem. Commun*., **48**, 10529–10530 (2012).

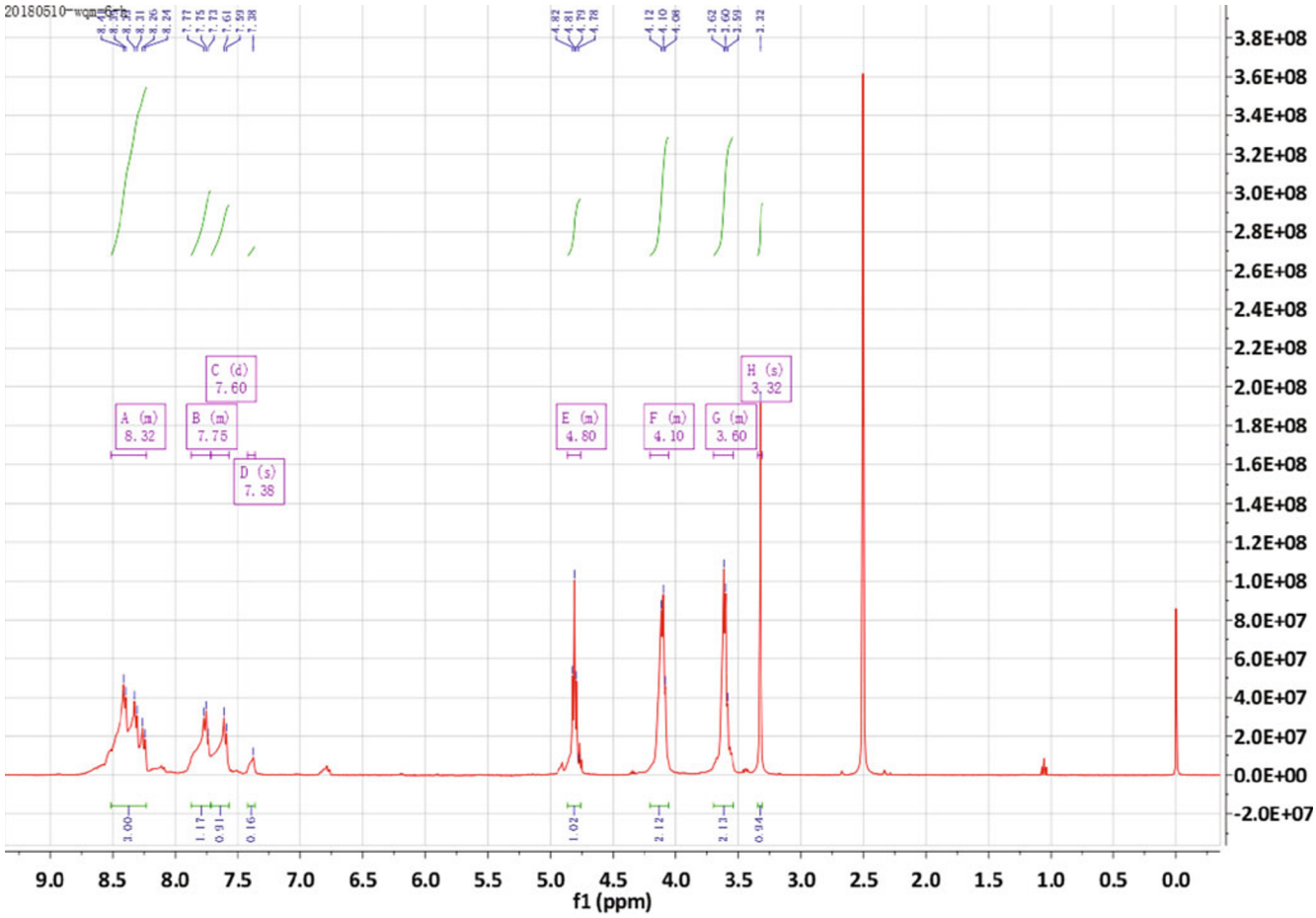

Fig. S1. ^{1}H NMR spectrum of probe.

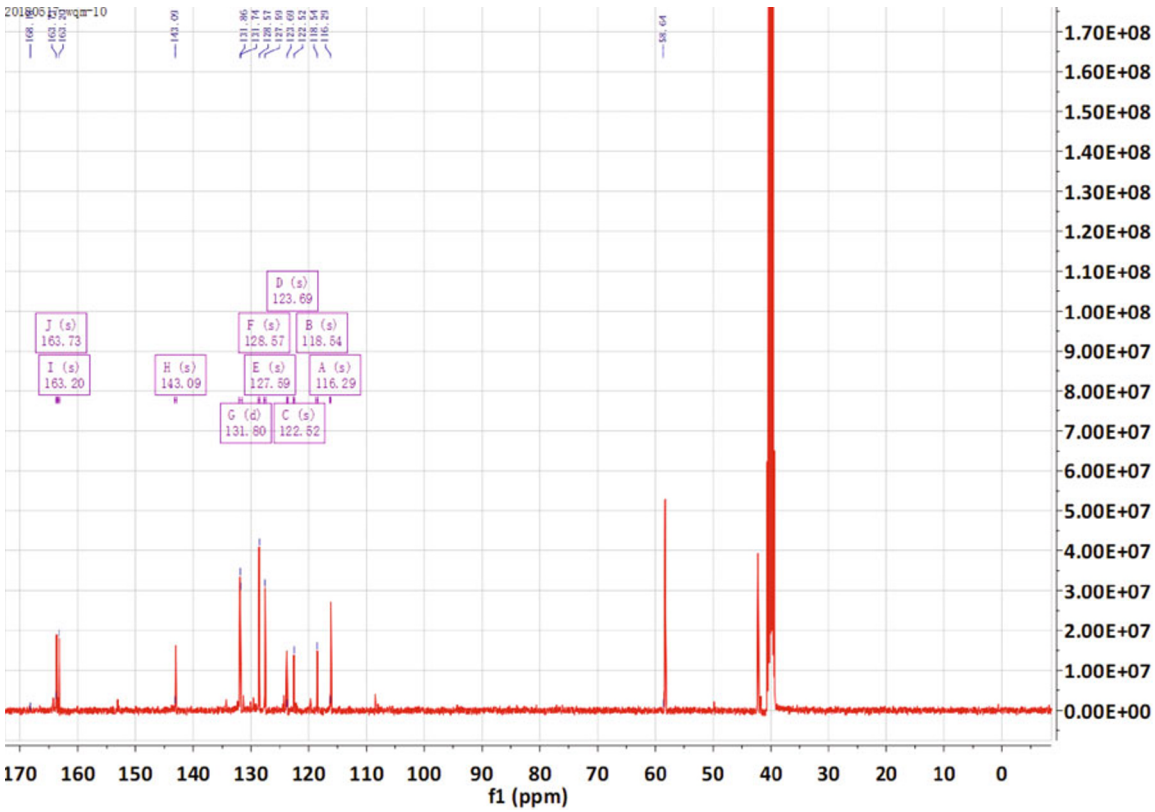

Fig. S2. ^{13}C NMR spectrum of probe.

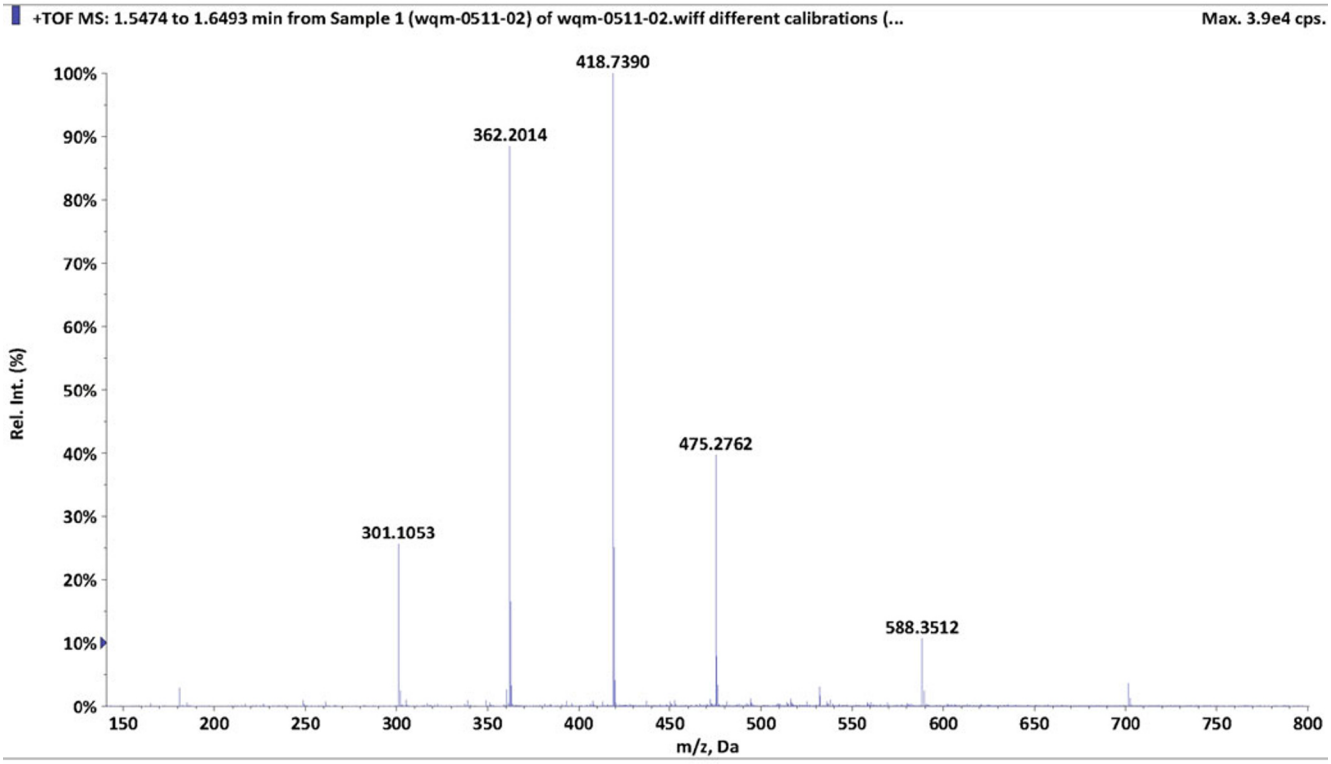

Fig. S3. Electrospray ionization mass spectrometry of probe.

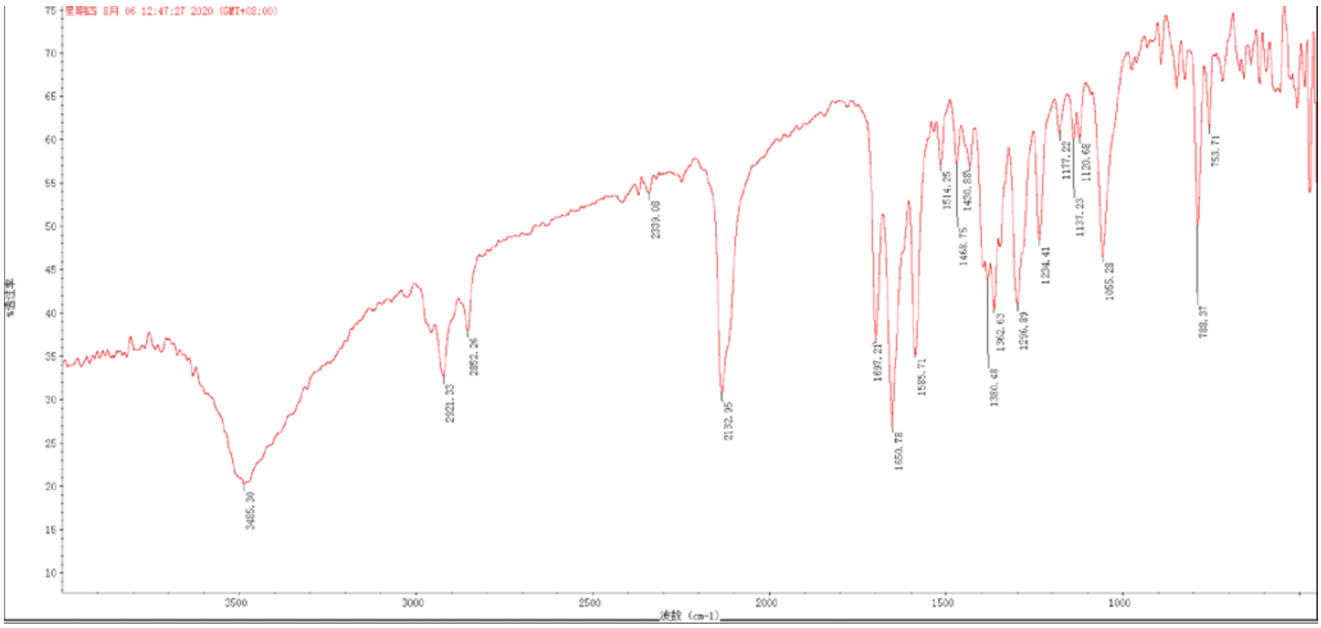

Fig. S4. Infrared spectra of probe.